Please cite the Published Version

Assessing the Asymmetric Effect of Global Climate Anomalies on Food Prices: Evidence from Local Prices

Lotanna E. Emediegwu[1]

Abstract

This paper uses time-varying smooth transition autoregressive model to investigate the asymmetric nature of El Niño Southern Oscillation (ENSO) —an exogenous climatic factor—with respect to the nonlinear dynamics of food prices in sub-Saharan Africa. Curating food price series from more than 1100 markets from 36 SSA countries, the study finds that ENSO (linearly or nonlinearly) affects roughly half of food prices considered, with most nonlinear models exhibiting strong asymmetric properties with shock-inflicted persistence. Moreover, in terms of the location of the burden of ENSO impact, I find a geographical and food product divide. Specifically, ENSO appears to be more efficacious on maize prices in Southern, Eastern, and some parts of Central Africa. Conversely, local rice, cassava, millet, and animal products are least affected. The policy implication of this dichotomy is that response to ENSO news should be subregion-specific rather than region-specific, depending on how the subregions absorb the shock.

1 Introduction

Eradicating food insecurity remains one of the major goals of world leaders, as it combines with ending hunger, improving nutrition, and promoting sustainable agriculture to form the second goal in the Sustainable Development Goals (SDGs). While this problem is a global issue, it is generally agreed that the threat is greatest in developing regions, like sub-Saharan Africa (SSA), where 23% of the people are malnourished (UN 2017b). Part of the reasons for such, as iterated in the UN Secretary-General's report, is due to the high or moderately high domestic prices for one or more primary cereal food products (UN 2017a).

A surge in food prices (however short-lived) is a vital feeder of risk in low-income food-deficit economies. Raising prices in a situation of limited substitution where the poor

✉ Lotanna E. Emediegwu
  l.emediegwu@mmu.ac.uk

[1] Department of Finance and Economics, Manchester Metropolitan University, Manchester, UK

spend majority of their income on food can seriously affect the welfare of the poor, plunge a multitude into poverty, and increase the number of people requiring food aid.[1] Numerous studies have documented the significant impact of climate variability on food prices. For instance, d'Amour et al. (2016); Wheeler and Von Braun (2013) assert that climate shocks, such as droughts and floods, can cause substantial fluctuations in crop yields, leading to price volatility in global food markets. Similarly, Cottrell et al. (2019) illustrate that the frequency and intensity of these climatic events are projected to rise with global warming, exacerbating food price instability and threatening food security. However, the question remains: do global climate shocks affect food price dynamics in Africa?

Given that high food prices affect the quantity and quality of consumption, as well as spending in general, the resulting food insecurity can lead to violent protests, thereby escalating local, regional, and global insecurity (McGuirk and Burke 2020; Bellemare 2015). Moreover, price volatility makes the income of food producers and others in the food supply chain uncertain and the consumer's expenditure unpredictable (Emediegwu and Nnadozie 2022). Consequently, the ability to analyse and forecast food prices is fundamental for a functional policy-making mechanism, especially in African countries, many of whom depend substantially on the exports of a small number of primary commodities (Deaton 1999).

Various studies have linked the behaviour of food prices in Africa to several covariates, such as global oil prices (e.g., Fowowe (2016); Dillon and Barrett (2015)); international food prices (e.g., Emediegwu and Rogna (2024); Minot (2014)); biofuels demand (e.g., Gilbert and Morgan (2010)); global factors (e.g., Tabe-Ojong et al. (2023); Agyei et al. (2021)); monetary and macroeconomic factors (e.g., Kargbo (2000)). Whereas the factors mentioned above appear to be robust correlates of African food prices, their impacts do not directly influence food production, except for biofuel demands.[2] This paper addresses this gap by analysing the implication of El Niño Southern Oscillation (ENSO), a food production-related factor on food prices in Africa. The importance of such medium-frequency climate anomalies (deviations from normal climate conditions) in the region has not received adequate attention in empirical studies. This paper intends to research in that direction.

The second contribution in this paper is in terms of the methodology employed. I utilise a regime-switching method to account for both nonlinearity and structural instability, two critical features of prices, especially when observed over long time spans. Previous studies focusing on African food price behaviour use standard linear models to investigate price behaviour. One main shortfall inherent in these econometric strategies is the assumption of a linear relationship between commodity prices and some exogenous variations, such as ENSO signals. Moreover, these models are inadequate for representing ENSO cycles as there is increasing evidence that indicates ENSO cannot be modelled by linear dynamics, as the impact of teleconnection may not necessarily be symmetric since climatic conditions in a location can be correlated with one phase of ENSO and not the other (Ubilava 2017; Hsiang et al. 2011). Furthermore, there is compelling evidence from Balagtas and Holt (2009); Deaton (1999); Deaton

---

[1] Although it can be argued that rising food prices will raise the income of farmers or labourers who supply them; however, the rise will also decrease the real income of all households through consumption (see, Bazzi and Blattman (2014)).

[2] The impact of variation in biofuel production on food prices is more remarkable in the international market and not in developing economies like SSA, where the current biofuel production is low, mainly due to the high cost of producing and processing biofuels (see, Ajanovic (2011); Zhang et al. (2010); Headey and Fan (2008)).

and Laroque (1992) that the behaviour of many agricultural commodities prices follows a nonlinear regime dependence. For these reasons, standard linear models may not correctly model the relationship between ENSO activities and price movements. Consequently, this work leverages Lundbergh et al. (2003) time-varying smooth transition autoregressive (TV-STAR) model to investigate the asymmetric nature of ENSO in relation to the nonlinear dynamics of food prices in SSA, as well as to further control for potentially complex dynamic relationships between the two variables.

Lastly, a key improvement over earlier African studies is in the set of local price information used. I constructed a new database of food prices for SSA, one with more than 60 per cent more food-country data than preceding sources - in terms of commodity, temporal and spatial coverage. Overall, this paper examines 188 price series from more than 1100 markets from 36 SSA countries covering 14 staple foods. In principle, I disaggregate the impact of ENSO shocks into country-commodity classes, given that ENSO shocks may exert heterogeneous effects amongst several food products and across countries, an aspect ignored by previous research. The importance of considering several commodities stem from the observation of Deaton (1999, p. 25): "*… prices of different commodities do not move in parallel. Although fluctuations in world demand impart common components to many price series, supply conditions differ across goods, and relative prices are far from constant.*" Moreover, given the influence of food price shocks on household and national income, local food prices provide a better-measured, more robust and plausible proxy of high-frequency variation in income (Bazzi and Blattman 2014). These features further reinforce the importance of understanding the dynamics behind food price swings.

I summarise my findings as follows. In terms of model selection, nonlinearity is not rejected for 22% of the food price series, and parameter constancy is rejected for 11% of the sample. However, 3% of the price series allows for concurrent nonlinearities and time-varying parameters. Overall, I find that ENSO (linearly or nonlinearly) affects roughly half of food prices considered. Besides, most of the nonlinear estimation models exhibit strong asymmetric properties with shock-inflicted persistence, which appear not to converge over the simulation period. Hence, the dynamics arising from an El Niño shock differs from those occasioned by a La Niña disturbance, justifying the need to use nonlinear models to analyse food prices in Africa. Lastly, regarding the location of the burden of ENSO impact, I find a geographical and food product divide. For example, ENSO appears to be more effective in Southern, Eastern, and some parts of Central Africa, while the effect is subdued in the Western African subregion. On the other hand, prices of weather-tolerant food products such as millet and cassava appear to be more stable than those of climate-sensitive food products like maize and sorghum. The policy implications arising from this contrast suggest that responses to ENSO news should be tailored to subregions rather than applying a uniform approach, contingent upon the varying capacities of subregions to absorb the shock.

The remainder of this paper is adumbrated as follows. The next Section clarifies some conceptual notions and causal mechanisms. Section 3 describes the model and data. The results are discussed in Sect. 4, while Sect. 5 summarises the paper with relevant policy implications.

2 Conceptual Clarifications and Transmission Channels

2.1 El Niño Southern Oscillation (ENSO)

The El Niño Southern Oscillation (ENSO), a cyclical and quasi-periodic event that occurs every few years in the tropical Eastern Pacific Ocean, consists of a neutral or normal phase and two extreme phases, El Niño and La Niña. In the neutral phase, the trade winds, known as "easterlies", blow from east to west across the surface of the tropical Pacific Ocean, pushing warm surface water from South America to Asia and Australia. The temperature variation from climatology is within 0.5 °C, and close to half of all years are within this period. These patterns in the Pacific are periodically disturbed by some forms of abnormal atmosphere-ocean interactions. El Niño denotes a positive deviation and causes an abnormally higher sea-surface temperature (SST), weakening or reversing the easterlies, making them "westerlies". On the other extreme, La Niña is a negative deviation from the normal, intensifying the easterlies motion and resulting in abnormally cold seawater across the Pacific.[3] These heterogeneous effects are summarised in Table 1, whereas Figure A3 in the Appendix illustrates the movement of the trade winds for the two ENSO states.

Although these episodes occur in the Pacific Ocean, they affect and can magnify weather conditions in various regions and countries around the globe: a phenomenon known as "teleconnection" in climate literature (see, Figure A4 in Appendix). Consequently, they have profound implications for economic outcomes. In their conflict studies, Hsiang et al. (2011) show empirically that weather patterns in SSA and some other parts of the world are strongly affected by ENSO events in the Pacific.[4] Above all, the 2015/2016 ENSO event (also known as the "Godzilla" due to its severity) caused severe droughts in some parts of SSA, such as Ethiopia, and flooding in the Horn of Africa. These severe weather conditions, in turn, resulted in catastrophic disruption of agricultural production and fish lives (FAO 2017).

2.2 Food Price Behaviour and ENSO - the Channels

ENSO shocks can impact food prices directly or indirectly through several channels. While the direct effects are primarily from supply-side channels, the indirect effects are demand-side. From the supply side, which constitutes the most important bunch of channels, Ubilava and Abdolrahimi (2019); Hsiang and Meng (2015), in separate papers, find that agricultural activities are tightly coupled to ENSO state. Their results further reveal that these effects are more pronounced in ENSO-teleconnected areas, such as SSA economies. Similarly, Iizumi and Ramankutty (2015) assert that staple foods, such as rice, wheat, and maize, often experience significant price volatility due to ENSO events, primarily because these crops are highly sensitive to changes in weather patterns. In the case of processed foods, which include items like cooking oil and packaged snacks, their prices can be affected directly by the raw materials' price volatility due to ENSO-related

---

[3] El Niño is Spanish for " the boy", and the capitalised term refers to the child, "Christ Jesus", because periodic warming in the Pacific near South America is usually noticed around Christmas. The name, La Niña, originates from Spanish, meaning " the girl".

[4] Hsiang et al. (2011) construct a global partition of ENSO teleconnection (that is, dividing the world into "teleconnected" and "weakly affected" areas) by examining whether reanalysis weather grid cells exhibit surface temperatures that are positively correlated with NINO3 on a monthly basis (with a two month lag) for at least three months of the year. See their paper for technical details.

agricultural disruptions. Further, prices of animal products such as meat, dairy, and eggs can be impacted directly by extreme weather conditions, which can reduce pasture quality and water availability, leading to lower livestock productivity (Emediegwu and Ubabukoh 2023). Given the foregoing evidence, it is expected that unanticipated changes in the supply side of the food market can push commodity prices temporarily out of equilibrium, thereby generating nonlinearity in the price series (see, Deaton and Laroque (1992)). Consequently, large price swings are mainly piloted by supply shocks, which could be influenced by crop productivity.[5]

Considering the indirect impacts, Deaton (1999) asserts that demand-side fluctuations are also major causes of commodity price volatility. ENSO can, therefore, affect food prices by influencing any demand-side channel. For example, Callahan and Mankin (2023); Smith and Ubilava (2017) find that El Niño persistently reduces country-level GDP growth, which is also analogous to the findings of Dell et al. (2012); McArthur and Sachs (2001) that developing countries are poor due to geographical factors (e.g., climate).[6] Similarly, Cashin et al. (2017) find that an El Niño occurrence has an adverse macroeconomic effect vis-à-vis fall in economic activities and short-run inflationary pressures. Hence, these knock-on effects on economic growth following global climate fluctuations may generate demand-shocks that can affect food prices negatively. For example, a fall in GDP per capita may affect demand for staple food adversely (depending on the elasticity, however), which may cause suppliers to reduce food prices, especially for perishable food products (Emediegwu and Nnadozie 2022). Furthermore, conflict arising from ENSO cycles (e.g., Hsiang et al. 2011) can also constitute another demand-related channel through which global climate anomalies can affect food prices. For example, household incomes can be affected following destruction of lives and livelihood, which may result in a fall in derived demand, thereby snowballing into a fall in food prices. It is important to state that the above-stated indirect impacts affect food groups similarly. For instance, a disruption in supply chain due to conflict would affect market stability and pricing for staple, processed, and animal product foods alike.

To sum up this subsection, there are several channels through which ENSO shocks can influence food prices. However, the intention of this paper is not to quantitatively determine the individual contributions of each channel; rather, a reduced-form framework is employed to analyse the general pass-through effect of ENSO on food prices in SSA.

3 Data and Model Specification

3.1 Econometric Strategy

This subsection describes the empirical technique used in this paper for modelling the nonlinear dynamic relationship between ENSO and food prices in sub-Saharan Africa. I adopt the time-varying smooth transition autoregressive (TV-STAR) modelling framework developed by Lundbergh et al. (2003) as the main empirical strategy to

---

[5] Domestic food prices follow local production; however, for imported staple food like rice, the fluctuation in prices comes from the exporting country's agricultural condition. Whichever the case, the point is that the price volatility can be supply-driven, either from home or abroad.

[6] Another school of thought pioneered by Acemoglu et al. (2001) attributes the lack of economic growth in developing economies to the role of institutions. While not discounting other causes, we contribute to the scientific debate by examining the cause of economic growth from a geographical perspective.

Table 1 Impacts of ENSO states

El Niño	La Niña
Warmer SST	Colder SST
Occurs every 3–8 years	Unknown frequency
Wetter than normal summers	Drier than normal summers
Weak trade winds	Strong trade winds
Fewer Atlantic hurricanes	Increased hurricanes in the Atlantic

capture regime-dependent nonlinearities and structural changes simultaneously in food price response to ENSO shocks. This model is a variant of Teräsvirta's (1994) smooth transition autoregressive (STAR) model.

I proceed by presenting a generalised time series model that allows for only nonlinearities, that is, a STAR model,

$$y_t = \boldsymbol{\varphi_0'} \boldsymbol{x_t} + \sum_{j=0}^{K} \boldsymbol{\varphi_j'} \boldsymbol{x_t} \mathbb{H}_j(\kappa_{j,t}; \boldsymbol{\Theta_j}) + \varepsilon_t, \quad t = 1, ..., T \tag{1}$$

where y_t is the outcome variable observed at times $t = 1 - p, -p, \ldots, -1, 0, 1, \ldots T - 1, T$; $\boldsymbol{x_t} = (1, y_{t-1}, ..., y_{t-p}, z_{1,t}, ..., z_{n,t}, r_{1,t}, ..., r_{n,t})'$ is a set of explanatory variables, which, respectively, includes lagged endogenous, exogenous ($z[.]$), and deterministic variables plus seasonal dummies ($r[.]$), where p is the autoregressive order; $\boldsymbol{\varphi_j} = (\alpha_j, \beta_{j1}, ..., \beta_{jp}, \gamma_{j1}, ..., \gamma_{jn})'$ are vectors of parameters to be estimated; ε_t is a white noise process. $\mathbb{H}_j(\kappa_{j,t}; \boldsymbol{\Theta_j})$ is a transition function where $\kappa_{j,t}$ is the state variable that regulates transition by determining the state of nature at time t, and Θ_j is a vector of parameters associated with the transition function, where $j = 0, ..., K$ is the number of transition functions in the model.[7] The transition variable can take several forms: a lagged endogenous variable ($\kappa_t = y_{t-d}; \exists \, d > 0$), an exogenous variable ($\kappa_t = z_t$), or a nonlinear function of the first two forms or time. The transition variable in this work will take the form of an exogenous variable (refer to subsection 3.3 for more discussion).

Restricting $\mathbb{H}_j(\kappa_{j,t}; \boldsymbol{\Theta_j})$ can transform (1) into several autoregressive (AR) models. For example, constraining $\mathbb{H}_j(\kappa_{j,t}; \boldsymbol{\Theta_j}) = 0$ will reduce (1) to a linear AR(p) model.[8] On the other hand, a more restricted (Tsay 1989) and Tong (1990) threshold autoregressive (TAR) model will result if $K = 1$ and $\mathbb{H}_j(\kappa_{j,t}; \boldsymbol{\Theta_j}) = \{0, 1\}$. In this case, the transition function plays the role of an indicator function. Further, if $K = 1$ and $\mathbb{H}_j(\kappa_{j,t}; \boldsymbol{\Theta_j}) = [0, 1]$, the transition function assumes a continuous function bounded between 0 and 1, resulting in Teräsvirta's (1994) smooth transition autoregressive (STAR) model exemplified in Eq. (2)

$$y_t = \boldsymbol{\varphi_0'} \boldsymbol{x_t} (1 - \mathbb{H}(\kappa_t, \eta, \rho)) + \boldsymbol{\varphi_1'} \boldsymbol{x_t} \mathbb{H}(\kappa_t, \eta, \rho) + \varepsilon_t \tag{2}$$

where η is speed-of-adjustment or smoothness parameter that governs the occurrence of regime shifts, and ρ is location parameter that dictates the value(s) of κ_t that defines the symmetry of regime changes. The associated regimes can be thought of as two extreme

---

[7] Although it is possible to have a multiple-regime STAR (MRSTAR) model, the conventional practice in the literature is to keep the number of regimes restricted and simple. For example, a binary-regime model that distinguishes expansion from contraction is popular in the business cycle literature.

[8] Linear autoregressive models are considered the basic building block, as well as the most restricted form of the STAR model.

values of the transition function, $\mathbb{H}(\kappa_t, \eta, \rho) = 0$ and $\mathbb{H}(\kappa_t, \eta, \rho) = 1$ with smooth inter-regime transition. In principle, the pathway of y_t can be described as a weighted mean of two linear AR structures governed by the regime at time t, which, in turn, depends on the state parameter.

It is important to note that $\mathbb{H}(\kappa_t, \eta, \rho)$ can follow several specifications. The most commonly used, however, are the 1st-order logistic (forming the LSTAR model) and exponential (ESTAR model) functions which can be written, respectively, as

$$\mathbb{H}_{LSTAR}(\kappa_t, \eta, \rho) = [1 + \exp\{-\eta(\frac{\kappa_t - \rho}{\sigma_\kappa})\}]^{-1}, \ \eta > 0; \rho \in [\psi_{\kappa_t}, 1 - \psi_{\kappa_t}] \tag{3}$$

$$\mathbb{H}_{ESTAR}(\kappa_t, \eta, \rho) = 1 - \exp\{-\eta(\frac{\kappa_t - \rho}{\sigma_\kappa})^2\}, \ \eta > 0; \rho \in [\psi_{\kappa_t}, 1 - \psi_{\kappa_t}] \tag{4}$$

where σ_κ is the standard deviation of κ_t; the restriction $\eta > 0$ is an identification restriction; ψ_{κ_t} is the truncation factor normally pegged at the 15th and 25th percentile of the transition variable in (3) and (4), respectively. Normalising η by σ_κ renders the former unit-free.[9] The LSTAR model denotes that the regimes of the transition variable, κ_t, possess different dynamics and are associated with high and low values of κ_t relative to the threshold parameter, ρ, as shown in Fig. 1. Conversely, the ESTAR model indicates that shocks move from high or low levels towards the middle ground in an analogous manner; hence, the regimes are associated with the absolute high and low values of κ_t. Moreover, the Figure also shows that the logistic function switches monotonically from 0 to 1 as κ_t increases from small to large values, with the change centred around ρ. Also, depending on the value of the smoothness parameter, η in the logistic function $\mathbb{H}(\kappa_t, \eta, \rho)$, the STAR model can approach certain sub-models. For example, as η becomes larger, the logistic function $\mathbb{H}(\kappa_t, \eta, \rho)$ approximates a dummy function, $I[\kappa_t > \rho]$; therefore, the transition between the two regimes becomes instantaneous rather than gradual. Where the above is the case, (3) and (2) reduce to a two-regime threshold autoregressive (TAR) model.[10] On the other extreme, as $\eta \to 0$, $\mathbb{H}_{LSTAR}(\kappa_t, \eta, \rho) \to 0.5$, and in the limit, (2) reduces to a linear AR model. The choice of ESTAR against LSTAR is also predicated on the Lagrange multiplier (LM) test.

Lastly, where $K = 2$, indicating the presence of two transition functions in the model, one of which is time-varying, (1) will metamorphose into a TV-STAR model (as in (5))

$$
\begin{aligned}
y_t = &[\boldsymbol{\varphi}_0' \boldsymbol{x}_t (1 - \mathbb{H}_1(\kappa_t, \eta, \rho)) + \boldsymbol{\varphi}_1' \boldsymbol{x}_t \mathbb{H}_1(\kappa_t, \eta, \rho)][1 - \mathbb{H}_2(\tilde{t}, \eta_\varsigma, \varsigma)] + \\
&[\boldsymbol{\varphi}_2' \boldsymbol{x}_t (1 - \mathbb{H}_1(\kappa_t, \eta, \rho)) + \boldsymbol{\varphi}_3' \boldsymbol{x}_t \mathbb{H}_1(\kappa_t, \eta, \rho)] \mathbb{H}_2(\tilde{t}, \eta_\varsigma, \varsigma) + \varepsilon_t
\end{aligned}
\tag{5}
$$

where $\tilde{t} = t/T$ and $\varsigma \in [\psi_{\tilde{t}}, 1 - \psi_{\tilde{t}}]$; other notations are already defined above.[11] The implication of (5) is that y_t is described as a STAR model at all times, however, with smoothly changing AR parameters from $\boldsymbol{\varphi}_0$ to $\boldsymbol{\varphi}_2$ for $\mathbb{H}_1(\kappa_t, \eta, \rho) = 0$, and from $\boldsymbol{\varphi}_1$ to $\boldsymbol{\varphi}_3$ for $\mathbb{H}_1(\kappa_t, \eta, \rho) = 1$. In the likeness of the STAR model, estimation of the parameters of

---

[9] Van Dijk et al. (2002); Teräsvirta (1994) reveal that the importance of normalising η by σ_κ is to prevent the former from certain estimation problems, such as overestimation and slow convergence.

[10] $\kappa_t = y_{t-d}$ presents a special case of self-exciting TAR (SETAR) model, which is extensively detailed in Tong (1990) for interested readers.

[11] κ_t determines the specification $\mathbb{H}(\kappa_t, \eta, \rho)$ follows. For example, if κ_t is specified as some function of lagged values of y_t or an exogenous explanatory variable (as in this case), then the transition function will follow either the LSTAR or ESTAR specification. However, if κ_t is specified as a function of time, then a model with smoothly changing parameters will result.

a TV-STAR model is *via* nonlinear least squares (NLS) (see, Lundbergh et al. (2003) for more econometric insights). However, determination of the appropriate (non)linear model is based on Lundbergh et al. (2003); Teräsvirta (1994); Granger and Terasvirta (1993) testing approaches, which depend to a large extent on the use of Lagrange multiplier (LM) tests, which are described in Section A of the Appendix.[12]

3.2 Data Sources and Description

3.2.1 Food Prices Data

I construct a new database of food prices for SSA, one with more than 60% more country-food data than prior sources—both in terms of temporal and spatial coverage. The primary source of the monthly food prices is from food price dataset products provided by United Nations agencies (the World Food Programme (WFP) and the Food and Agriculture Organization (FAO)). The WFP dataset covers staple and processed foods such as maize, rice, beans, fish, and sugar for 76 countries[13] and some 1500 markets, while the FAO Global Information and Early-Warning System (FAO GIEWS) dataset presents over 1200 price series for 89 countries. The data goes back as far as 1992 for a few countries, although many countries started reporting from 2003 or thereafter. To update missing countries and years, I use food prices from additional sources—Famine Early Warning System Network (FEWS-NET) and the Association for Strengthening Agricultural Research in Eastern and Central Africa and Regional Strategic Analysis and Knowledge Support System (ASARECA/ReSAKSS).[14] The former dataset contains monthly staple food price data collected by FEWS-NET since 1995, but the latter was collected from primary and secondary sources from several project partners in the Eastern African subregion with funding from the World Bank Multi Donor Trust Fund (MDTF) under ASARECA.[15]

Overall, my sample contains 188 monthly price series from 1168 markets from 37 of 46 SSA countries (excluding countries with less than ten years of food price data) covering 14 staple foods (see, Fig. 2). Higher frequency data are not available. The sample includes prices of staple, processed and animal product foods to explore whether the effect of ENSO differs for different food classes (see Table A1 in the Appendix for locational, economic, market and distributional details of commodities sampled).[16] [17] The choice of food products is based on data availability and significance, in the sense that they can be stored for longer periods; ergo, they are the focus of governments efforts to mitigate food price instability (Minot 2014). Given the importance of retail food prices to household welfare, most

---

[12] Lundbergh et al. (2003) expanded Teräsvirta (1994); Granger and Terasvirta (1993) approach to allow for time-varying parameters.

[13] About 50 per cent are SSA countries.

[14] https://data.humdata.org/dataset/eastern-africa-food-prices-data

[15] In 2014, however, funding from MDTF ended, but ReSAKSS continued updating the dataset.

[16] The food items considered are beans, bread, cassava, maize, millet, meat, milk, imported rice, local rice, potato, sorghum, sugar, wheat, and vegetable oil.

[17] Even though the sample selection was with respect to data availability, the countries in my sample represent about 80 per cent of SSA countries drawn from the various subregions. The remaining countries were not used due to inavailability of data.
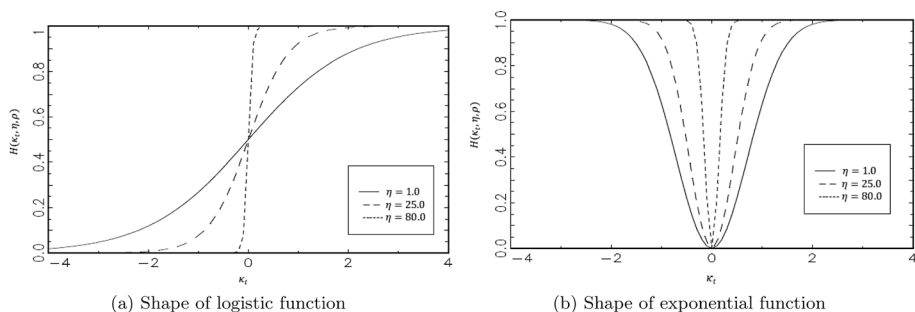
(a) Shape of logistic function

(b) Shape of exponential function

Fig. 1 Examples of the transition functions $\mathbb{H}(\kappa_t, \eta, \rho)$ as described in Eqs. (3) and (4) for different values of the speed-of-adjustment parameter, η, at zero threshold ($\rho = 0$)

of the food prices were collected at the retail level except for Ghana and Ethiopia, where wholesale prices are used in the absence of adequate retail price data.[18]

This study cannot discountenance the possibility that the dataset could have omitted markets where prices are high due to some localised events, like conflict (Raleigh et al. 2015). However, such would not have been the case for the following reasons. One, several technical documents from the various data sources do not indicate omission of markets on the basis of factors such as conflict. Second, the Law of One Price necessitates that prices will eventually converge when the status quo is restored, even when discrepancies occur due to local conditions. Moreover, as shown in Narciso (2020), events like conflict or climate crises can result in migration, which eventually would reduce food prices due to fall in demand. Even where there is proof of sampling bias, such errors are exogenous to the explanatory variables, producing imprecise rather than biased estimates.

For each food commodity, each country's monthly ***Price***$_t$ is calculated as the national average of all market prices weighted by market population, where the population weights are the Year 2000 population count extracted from the Gridded Population of the World (GPWv4) dataset at 0.5 degree resolution (CIESIN 2018).[19] Using population as weight helps ensure that pass-through of the ENSO shocks funnels directly to the economy. I transformed the nominal prices (in local currencies) to their month-on-month (MoM) logarithmic values to ease the interpretation of the impulse responses in percentage terms.[20]

3.2.2 ENSO Index Data

ENSO indices based on the Southern Oscillation Index (SOI) and sea surface temperature (SST) are commonly used to correlate ENSO with prices (Cashin et al. 2017; Ubilava

---

[18] I ensure that the units of measurement for food prices across countries are denominated by a common unit as shown in Table A1 of the Appendix, although this has little consequence for my results.

[19] Few missing observations inherent in some of the price series are interpolated *via* cubic splines. The interpolation should not have a grave consequence on the analysis because the numbers of missing observations in the price series are petty, less than 10% of the data sample. To ensure much accuracy, series with missing observations for more than five consecutive months are not included.

[20] Most African countries do not have up-to-date monthly official exchange rates (local conversion units per US$), hence the use of prices in local currency as done in other studies (e.g., Dillon and Barrett (2015); Minot (2014)).
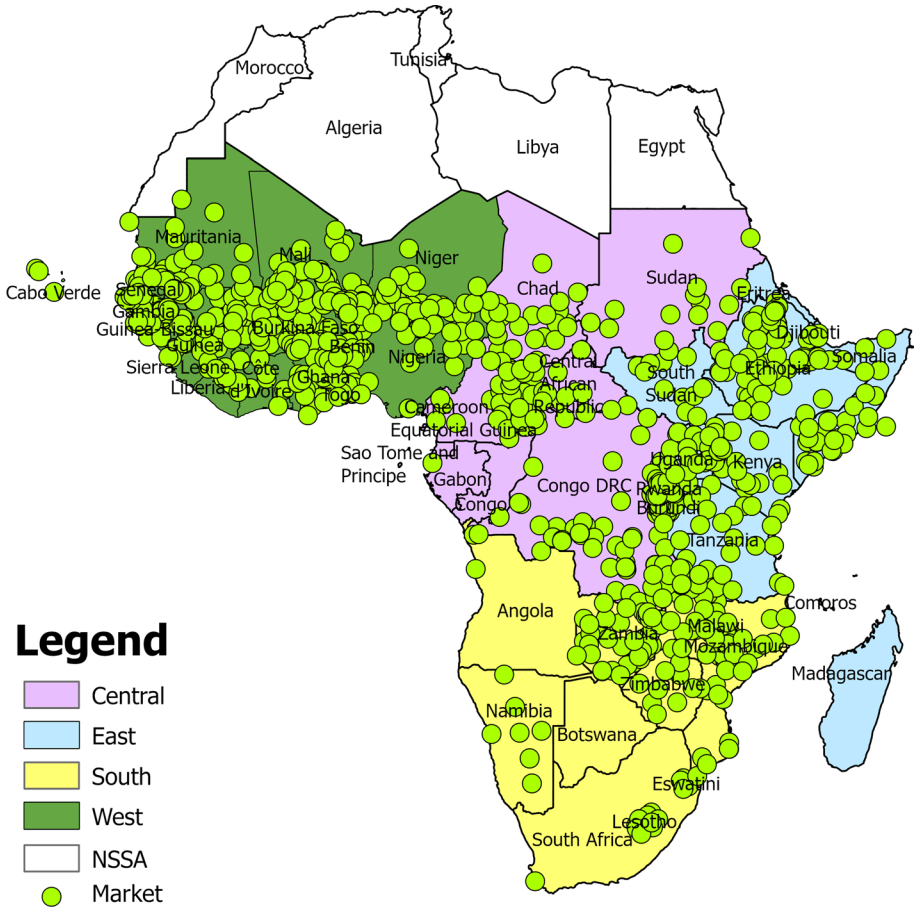
Fig. 2 Food Markets across sub-Saharan Africa. *Note*: Each green dot represents a local market where data for all the food commodities are collected

2017; Bastianin et al. 2016; Letson and McCullough 2001; Keppenne 1995). Given the multifaceted nature of ENSO, involving different aspects of the ocean and the atmosphere over the tropical Pacific, it is almost impossible to capture these in one measure, SOI or SST. Instead, multiple indices or a composite index can be used to deal with the various facets of ENSO. One such composite index used in this paper is the multivariate ENSO index (MEI).

The Multivariate ENSO Index (MEI) is based on the leading combined empirical orthogonal function (EOF) of five primary observed surface variables over the tropical Pacific basin (30°S–30°N and 100°E–70°W) —SST, sea level pressure, zonal and meridional components of the surface wind, and total cloudiness fraction of the sky. According to Wolter (1993), the MEI is derived as the first unrotated Principal Component (PC) of the above five observed variables computed separately over 12 sliding bi-monthly seasons, i.e., Dec/Jan, Jan/Feb, *etc*. Utilising and integrating Principal Component Analysis (PCA) across multiple variables allows the MEI to vary with the seasonal cycle, and the inclusion of more variables makes it less susceptible to instrumentation and reconstruction errors.

Thus, the MEI is more stable than most real-time indices of the El Niño Southern Oscillation (ENSO) and more efficiently captures its seasonality instead of geographically fixed, uni or bivariate indices such as SST, SOI, bivariate ENSO (Niño3.4 SST + SOI). Positive and negative values of MEI represent El Niño and La Niña, respectively.

MEI version 2 historical values are obtained from the National Oceanic and Atmospheric Administration's (NOAA) Earth System Research Laboratory.[21] An El Niño (a La Niña) phased ENSO cycle is said to occur if the MEI values exceed (in absolute terms) a threshold of +(-) 0.5 for five successive bi-monthly periods.[22] Given how noisy the MEI could potentially be with bi-monthly averaging, potential ENSO events wherein the aforementioned threshold-exceeding criterion is not met for just one singular bi-monthly period are also included as part of an entire El Niño or La Niña. Figure 3 shows MEI historical values alongside ENSO events. In Figure A5 and Table A2 of the Appendix, I show the high comovement that exists amongst MEI, SST and SOI, although MEI is more correlated with SST (0.90) than with SOI (0.78). Nevertheless, as robustness checks, I use SST and SOI to ascertain if the results are sensitive to the choice of ENSO index. A cursory investigation into Fig. 3 reveals that upturns (El Niño) occur more rapidly than downturns (La Niña), which indicate the potential existence of asymmetry in the data, thus necessitating the use of a regime-switching model in the present context.

3.3 Specification Tests and Models

In developing a TV-STAR model, it is highly recommended in the literature (see, Lundbergh et al. (2003)) that a systematic test-based approach should be followed to determine the requisiteness of the full model or a submodel, such as STAR, TAR, or AR model. Consequently, this study follows Granger's (1993) *specific-to-general* recommendation, starting with a simple AR model and building up to more complicated models only if diagnostics refutes the maintained model,[23] Additionally, selecting the appropriate delay parameter is also a data-based decision.

I start with a simple linear AR process for *Price* variable with MEI entering as an exogenous forcing variable[24]:

$$Price_t = \boldsymbol{\alpha}' \boldsymbol{x}_t + \varepsilon_t \tag{6}$$

where $\boldsymbol{x}_t = (1, Price_{t-1}, ..., Price_{t-v}, MEI_t, ..., MEI_{t-e}, , r_{1,t}, ..., r_{n,t})'$, $r_{j,t}, j = 1, ..., n$ are deterministic variables, which include monthly dummies; $\boldsymbol{\alpha}$ are estimable set of parameters, and ε_t is white noise process. v and e are dictated by sample-size-corrected Akaike information criterion (AICc). To avoid mistaking remaining residual autocorrelation for nonlinearity, I apply the Shapiro test to check for residual autocorrelations in the autoregressive distributed lag [ARDL](v,e) model selected by the AICc. This study follows the Augmented Dickey–Fuller (ADF) test for unit roots since the nonlinear test and use of (TV-STAR) model require stationary time series. Table A3 in the Appendix shows that the ADF test for

---

[21] https://www.esrl.noaa.gov/psd/enso/mei/

[22] By construction, MEI is unit-free.

[23] Although Lundbergh et al. (2003) query this approach and favoured an alternative, *specific-to-general-to-specific* they use Monte Carlo simulations to show that neither of the two approaches dominates the other.

[24] This assumption is hardly controvertible and widely supported by evidence (Blanc and Reilly 2017; Hsiang and Meng 2015; Brunner 2002)

most prices series follows unit root process (*I(1)*) where prices series will be differenced series: $\Delta Price = Price_t - Price_{t-1}$. In addition, this paper follows the standard practice in the climate econometrics literature (e.g., see Emediegwu and Ubabukoh 2023; Ubilava and Abdolrahimi 2019), where other time-varying controls are excluded from the model. However, given that the identification variable is exogenous to omitted variables, there is confidence that the model will not be biased due to the omitted variables (Blanc and Reilly 2017; Hsiang 2016).

This work adopts Lundbergh et al. (2003); Teräsvirta (1994); Granger and Terasvirta (1993) LM testing approach to ascertain the presence or otherwise of nonlinearity and parameter constancy in the model.[25] Decisions about the null hypothesis of linearity and parameter constancy can result in any of the four possible scenarios described in Table 2. First, if the tests reject both null hypotheses, I will estimate a TV-STARDL model as presented below.

$$Price_t = [\boldsymbol{\alpha'_0}\boldsymbol{x_t}(1 - \mathbb{H}(\kappa_t, \eta, \rho)) + \boldsymbol{\alpha'_1}\boldsymbol{x_t}\mathbb{H}(\kappa_t, \eta, \rho)][1 - \mathbb{H}(\tilde{t}, \eta_\varsigma, \varsigma)]+$$
$$[\boldsymbol{\alpha'_2}\boldsymbol{x_t}(1 - \mathbb{H}(\kappa_t, \eta, \rho)) + \boldsymbol{\alpha'_3}\boldsymbol{x_t}\mathbb{H}(\kappa_t, \eta, \rho)]\mathbb{H}(\tilde{t}, \eta_\varsigma, \varsigma) + \varepsilon_t \tag{7}$$

where the transition function, $\mathbb{H}(\tilde{t}, \eta_\varsigma, \varsigma)$, abbreviated as $\mathbb{H}(\tilde{t})$ here and everywhere else, can either be a logistic or an exponential function of $\tilde{t} = t/T$, depending on the data. The remaining parameters and variables are as defined previously. For the logistic function, I restrict the slope parameters, η, between 2 and 100, while for exponential functions, the slopes are restricted between one and ten.[26]

However, sub-models nested by (7) would be estimated where we fail to reject, at least, one of the null hypotheses as shown in Table 2. For instance, where only the null of parameter constancy or linearity is rejected, I will adopt a TVARDL or STARDL framework, respectively. Where we fail to reject both the null hypotheses, an autoregressive distributed lag (ARDL) model will be estimated. Summarily, the specification in this paper allows ENSO intensity as captured in MEI to be transmitted linearly and nonlinearly to food price dynamics.

4 Results and Discussion

4.1 Linearity and Parameter Constancy Tests

As stated in the previous section, the first step to estimating a nonlinear model is to test for nonlinearity and parameter constancy. For the sake of organisation, I present the results in the following order: I focus on the modelling results of one food price series, maize. The choice of maize is based on the following reasons: First, maize has the largest share of price series in my database ($\sim 20\%$), which includes most countries in my sample. Second, the models selected under maize prices cover all range of model possibilities (see Table A4 in the Appendix for summary of model selection by commodity and country). Lastly, maize is the primary and cheapest source of calories in most African countries; hence, a detailed analysis of its price behaviour is more important for policy making and economic

---

[25] Another reason for linearity testing is to provide estimates for the parameter delay, *d*.

[26] Slope values greater than the upper bounds in both functions will result in an instantaneous switch between regimes, resulting in a TAR model.
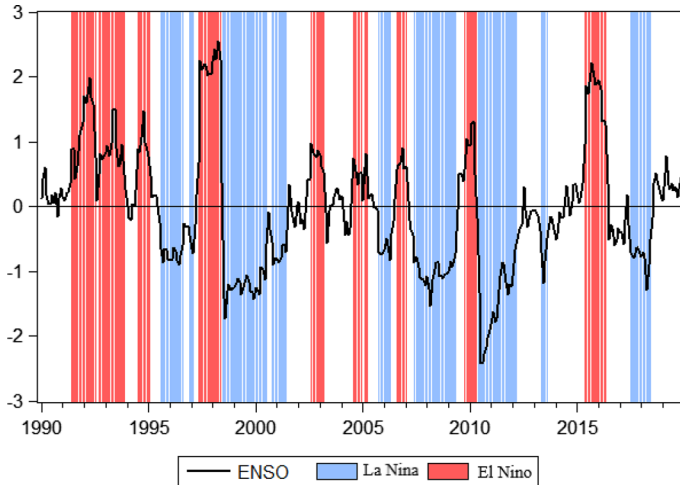
Fig. 3 MEI Values and ENSO Episodes (Bi-monthly Periods). *Note*: Red-coated regions represent observed El Niño regimes; the blue-coated regions represent observed La Niña regimes. Values above (below) + 0.5 (− 0.5) for five successive indicate occurrence of El Niño (La Niña) conditions. See in-text for more details

outcomes than other food commodities. Consequently, maize price series is used to glance at the estimated models and their evaluation. The model estimation and evaluation of other price series will follow hereafter.

4.2 Maize Price Series

Table 3 shows the selected models for maize prices in SSA countries, along with some inspection and diagnostics associated with the models. However, before turning to the asymmetric properties, let us first consider how ENSO affects maize prices across countries. The number of countries affected linearly or nonlinearly by ENSO and those unaffected are roughly divided into equal parts.[27] Fig. 4 displays a clear partition between countries affected by ENSO, mostly in the Southern, Central, and Eastern parts of Africa and those unaffected by ENSO in the Western subregion. The affected countries in my analysis coincide with areas with strong teleconnection to ENSO, as indicated in Figure A4 in the Appendix. The few countries in Eastern and Southern Africa, such as Tanzania, Namibia and Zambia, whose maize prices are not affected by ENSO, are classified as "highly-intervention" countries (Minot 2014). In these countries, the government intervenes actively in the maize market *via* marketing boards. Nonetheless, the extent to which these interventions absorb external shocks is a subject of debate. For example, some studies opine that government efforts to stabilise food prices may be counterproductive, especially under unpredictable commerce (see, Emediegwu and Nnadozie 2022; Deaton and Laroque 1996).

Although the few ENSO-affected countries in Western Africa are landlocked (with Ghana as an exception), there is no significant difference between landlocked and coastal countries, given that the impact of ENSO on local food prices passes through agricultural

---

[27] Here and elsewhere, unless otherwise stated, the use of "country" or "countries" is synonymous with the price series under consideration (maize prices in this instance) in the respective countries.

Table 2 Model selection based on hypothesis tests for linearity and parameter constancy

Rejected H_0	Model selected
None	AR(DL)
Linearity only	TVAR(DL)
Parameter constancy only	STAR(DL)
Both	TV-STAR(DL)

output.[28] Furthermore, the effects of ENSO on maize prices are more pronounced in countries with a rich history of conflict or political instability, such as Zimbabwe, DR Congo, Somalia, *etc.* The afore finding reinforces the submissions of Harari and Ferrara (2018); Hsiang et al. (2011) that ENSO fuels conflict *via* distortion of local weather, resulting in a decline in agricultural output. However, the mechanism through which ENSO affects prices in these conflict-prone areas is a subject for further investigation.

I now turn to the asymmetric properties of the estimated nonlinear models.[29] Angola, Ghana, Kenya and Niger follow a nonlinear ARDL process (LSTARDL), DR Congo and Somalia are characterised by structural changes (LTVARDL). Only Zimbabwe have maize price series that exhibit both nonlinearities and structural changes (LTV-LSTARDL). Given that the transition variable in the regime-dependent models is MEI, the estimated state parameter, $\hat{\rho}$ (reflecting the switching (or inflexion) point between the two ENSO regimes), and the estimated smoothness parameter, $\hat{\eta}_\rho$ (showing the velocity of the change in model dynamics from one regime to another) will be of interest. The estimates of the location parameters, $\hat{\rho}$, from the nonlinear models are significantly different from 0, which indicates that positive and negative changes in the series can be fairly characterised by states where $\mathbb{H}(.) = 0$ and $\mathbb{H}(.) = 1$, respectively. For more insight, Fig. 5 reveals the estimated transition functions for the nonlinear models, with values close to unity (zero) during El Niños (La Niñas). Furthermore, given the smooth cyclical nature of MEI, some delays longer than the selected distributed lags of MEI are observed in the price series response.[30]

The velocity of switch between the two regimes differs across models. For example, the value of $\hat{\eta}_\rho$ is low for Angola, meaning that the transition between regimes is smooth, as seen in Fig. 6. On the other hand, Kenya, Niger, and Zimbabwe have high values of $\hat{\eta}_\rho$, signalling that the transition from one regime to another is abrupt; hence, the model approximates a TAR(DL) model.[31] Following the insignificant estimates of some $\hat{\eta}_\rho$, I investigate

---

[28] Exposure to the sea (for coastal countries) means more access to wider market and may reduce the effect of ENSO on price volatility. However, this study finds no significant difference between coastal and landlocked SSA economies.

[29] Here, I only deal with nonlinear ARDL models.

[30] This delay is better understood in light that the selected transition variable for each univariate model is a lag (d) of MEI; hence, its fluctuations do not coincide with the turns in MEI.

[31] Suffice to note, as put forward by Lundbergh et al. (2003); Van Dijk et al. (2002), that large (or insignificant) estimates of the smoothness parameters are commonplace in regime-switching analysis because of (i) transition between different states is sharp for large values of κ_t; ergo, a large deviation in κ_t wields a negligible impact on the shape of the logistic function, (ii) few observations located in-between the two regimes for large values of κ_t. Hence, large standard error estimates of κ_t should not be taken as evidence against nonlinearity, rather, the models should be subject to further diagnostics check.

Table 3 Model selection, Inspection and residual diagnostics for maize price series

Country	Model	v	e	d	n	$\hat{\eta}_\rho$	$\hat{\rho}$	$\hat{\eta}_\zeta$	$\hat{\zeta}$	P_{PC}	P_{RA}	P_{ARCH}	AICc	$N\hat{\sigma}^2_\epsilon$
Eastern Africa														
Ethiopia	ARDL	2	1		16	16				0.22	0.45	0.58	0.165	1.18
Kenya	LSTARDL	3	11	5	54	100(127.88)	0.58 (0.14)			0.35	0.26	0.62	−0.133	0.42
Rwanda	AR	2			13					0.07	0.52	0.45	−0.296	0.71
Somalia	LTVARDL	1	7		44			4.12(1.44)	0.15 (0.04)	0.27	0.017	0.23	1.482	3.63
South Sudan	AR	3			14					0.09	0.61	0.40	2.017	6.96
Tanzania	AR	2			14					0.20	0.95	0.72	1.029	2.83
Uganda	ARDL	2	2		17					0.23	0.58	0.16	0.683	1.68
Central Africa														
Burundi	AR	1			14					0.40	0.16	0.10	0.143	0.99
Cameroon	AR	1			13					0.20	0.62	0.88	−0.469	0.64
CAR	ARDL	3	1		17					0.77	0.23	0.25	0.181	1.05
Chad	ARDL	2	6		21					0.89	0.75	0.99	−0.005	1.00
DR Congo	LTVARDL	1	2		34			19.61 (12.97)	0.85(0.02)	0.39	0.37	0.08	0.791	1.90
Southern Africa														
Angola	LSTARDL	2	1	0	32	2.36 (1.55)	0.53 (0.04)			0.69	0.16	0.75	−4.182	0.01
Eswatini	AR	1			12					0.67	0.98	0.13	−0.521	0.51
Lesotho	ARDL	2	1		15					0.63	0.78	0.48	−2.096	0.11
Malawi	AR	3			14					0.94	0.05	0.33	0.677	2.04
Mozambique	ARDL	3	1		17					0.41	0.17	0.41	0.813	2.07
Namibia	AR	2			13					0.18	0.31	0.69	−0.970	0.30
South Africa	ARDL	1	0		13					0.10	0.12	0.45	−0.678	0.60
Zambia	AR	1			13					0.26	0.05	0.33	0.760	2.04
Zimbabwe	LTV-LSTARDL	2	1	1	32	100 (135.58)	−0.45 (0.03)	100 (174.85)	0.15 (0.004)	0.85	0.35	0.29	1.853	12.17
Western Africa														
Benin	AR	1			12					0.08	0.14	0.16	0.414	1.43
Burkina Faso	ARDL	2	1		16					0.47	0.50	0.13	−0.328	0.73

Table 3 (continued)

Country	Model	v	e	d	n	$\hat{\eta}_\rho$	$\hat{\rho}$	$\hat{\eta}_\zeta$	$\hat{\zeta}$	p_{PC}	p_{RA}	p_{ARCH}	AICc	$N\hat{\sigma}_\epsilon^2$
Cape Verde	AR	1			12					0.09	0.49	0.06	−0.901	0.42
Côte d'Ivoire	AR	2			13					0.07	0.46	0.98	1.656	5.20
Ghana	LSTARDL	1	3	1	34	74.23 (26.55)	−1.06 (0.01)			0.33	0.16	0.08	0.554	1.36
Guinea-Bissau	AR	2			14					0.44	0.49	0.12	1.761	5.76
Mali	AR	1			12					0.83	0.22	0.63	0.702	2.04
Mauritania	AR	3			14					0.07	0.75	0.05	0.670	1.77
Niger	LSTARDL	6	7	0	52	41.85 (43.54)	−0.78 (0.02)			0.05	0.13	0.07	0.493	1.52
Nigeria	AR	1			13					0.05	0.62	0.97	0.952	2.32
Senegal	AR	1			13					0.89	0.15	0.13	−1.269	0.24
Togo	AR	1			13					0.68	0.05	0.46	0.840	3.28

v and e are the selected autoregressive and distributed lag lengths, respectively; d denotes the delay parameter of the transition function used to test for regime-dependency; $\hat{\eta}_\rho$ ($\hat{\eta}_\zeta$) and $\hat{\rho}(\hat{\zeta})$ respectively, represent estimated speed-of-adjustment and location parameters (values in parenthesis are standard errors). p_{PC}, p_{RA}, and p_{ARCH} represent the probabilities associated with hypothesis of (no remaining) parameter constancy, residual autocorrelation, and autoregressive conditional heteroskedasticity, respectively.

$AICc$, sample-size-corrected Akaike information criterion; $\hat{\sigma}_\epsilon$, residual standard deviation; N, sample size
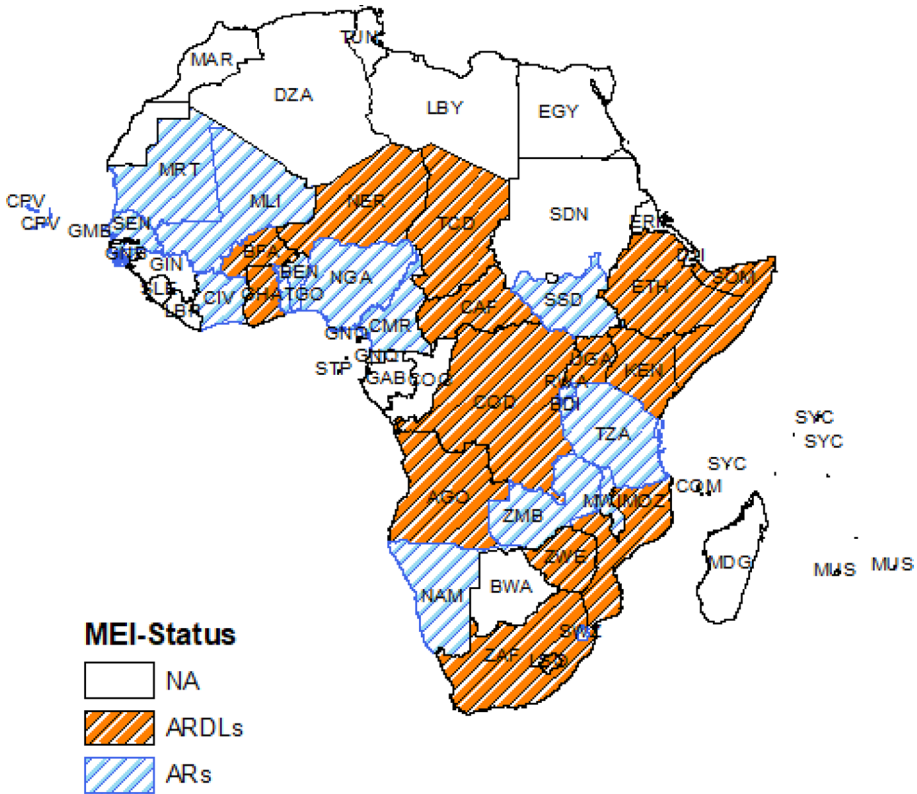
Fig. 4 Map of countries (un)affected by ENSO (Maize Prices). *Note*: Yellow (blue) stripes are countries whose maize prices are (not) affected by ENSO shocks

the diagnostics. Table 3 reveals that the conventional diagnostics for checking the appropriateness of a STAR model design are in order. For example, the associated *p*-values indicate that there are no remaining parameter constancy, residual autocorrelation or neglected heteroskedasticity (details of the computation of these tests are documented in Section A of the Appendix).

For time-varying models, the estimated location parameter, $\hat{\zeta}$ denotes the period in time around which the alteration of price dynamics occurs, while the estimated speed-of-adjustment parameter, $\hat{\eta}_\zeta$ indicates the time frame for the parameter change. The transition function of time (for TVARDL models only) reveals that the structural change is centred around $t/T = 0.85$ for DR Congo (corresponding to May 2017). This period follows after the most severe ENSO event of 2016, known as "Godzilla". For Somalia and Zimbabwe, the structural changes occur much earlier as they are centred around $t/T = 0.15$, corresponding to September 1998 and March 2007, respectively. Further, the speed of adjustment varies across countries. Somalia and DR Congo display relatively smooth changes, while Zimbabwe exhibits sharp transitions, as seen in Fig. 5. However, most of the changes are completed before the end of the sample period, with the exception of DR Congo. Note that the location parameters should be interpreted with care. They are at these values because of the restrictions imposed on the model
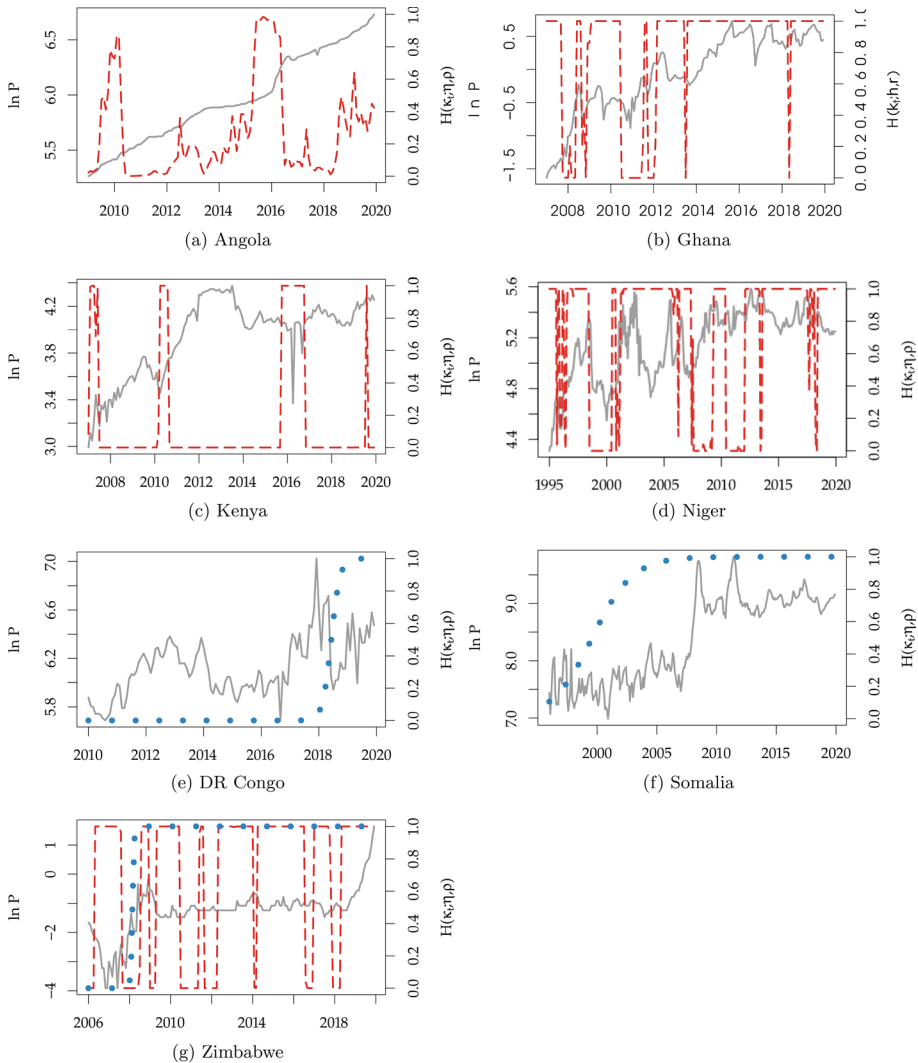
Fig. 5 Observed values and transition function versus time. *Note*: The Figure showcases the natural log of food price series, plus their associated estimated transition functions. The solid grey lines represent the series, the broken lines indicate the transition function of regime-dependent models over time, and time-varying transition function over time is denoted by the dotted line

to ensure enough observations are in each regime. In some cases, it may be difficult to pinpoint the "structural" reasoning behind the shift when combined with the smooth switch.

4.3 Dynamic Properties

Interpretation of the estimated parameters of a nonlinear model (except those in the transition function) is elusive. Ergo, one way of appreciating these models is to examine their
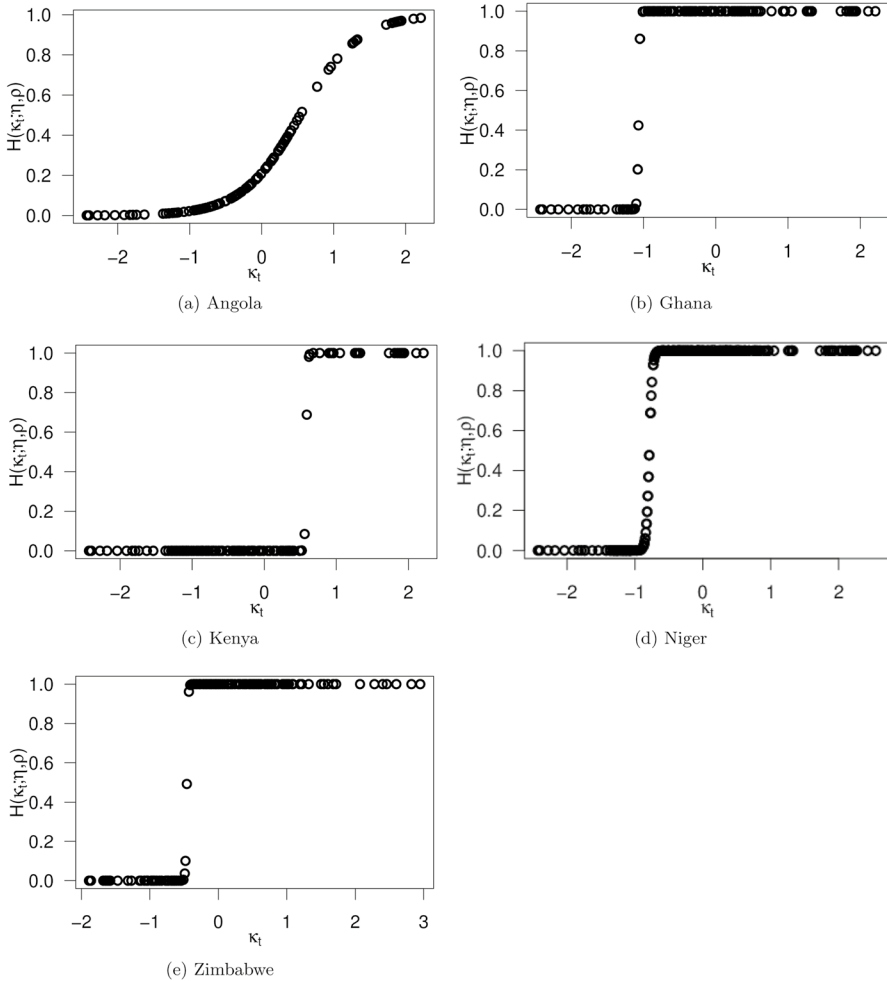
Fig. 6 Transition function versus transition variable. *Note*: Each dot represents one observation

dynamic behaviour - the persistence of shocks - over time *vis-a-vis* generalized impulse response functions (GIRFs), developed by Koop et al. (1996).[32] The computational details of the GIRFs are found in Section B of the Appendix.

Based on the counsel of Hyndman (1995; 1996) and the methods in Lundbergh et al. (2003), I employ 50%, 75% and 90% highest-density regions (HDRs) to represent the distribution of functions for 24 months ahead.[33] The estimated GIRFs, as presented in Figs. 7

---

[32] The use of GIRFs is occasioned by the invariance of nonlinear models to idiosyncratic shocks that may affect the underlying dynamics of a stochastic process. Consequently, the conventional extrapolation means of generating impulse-response functions (IRFs) for linear models is inapplicable in this case.

[33] HDR is a new form of boxplot developed in Hyndman (1995; 1996), which describes a distribution in a similar way as the boxplot with allowance for multimodality display. For example, the 50% HDR replaces the box bounded by the interquartile range.
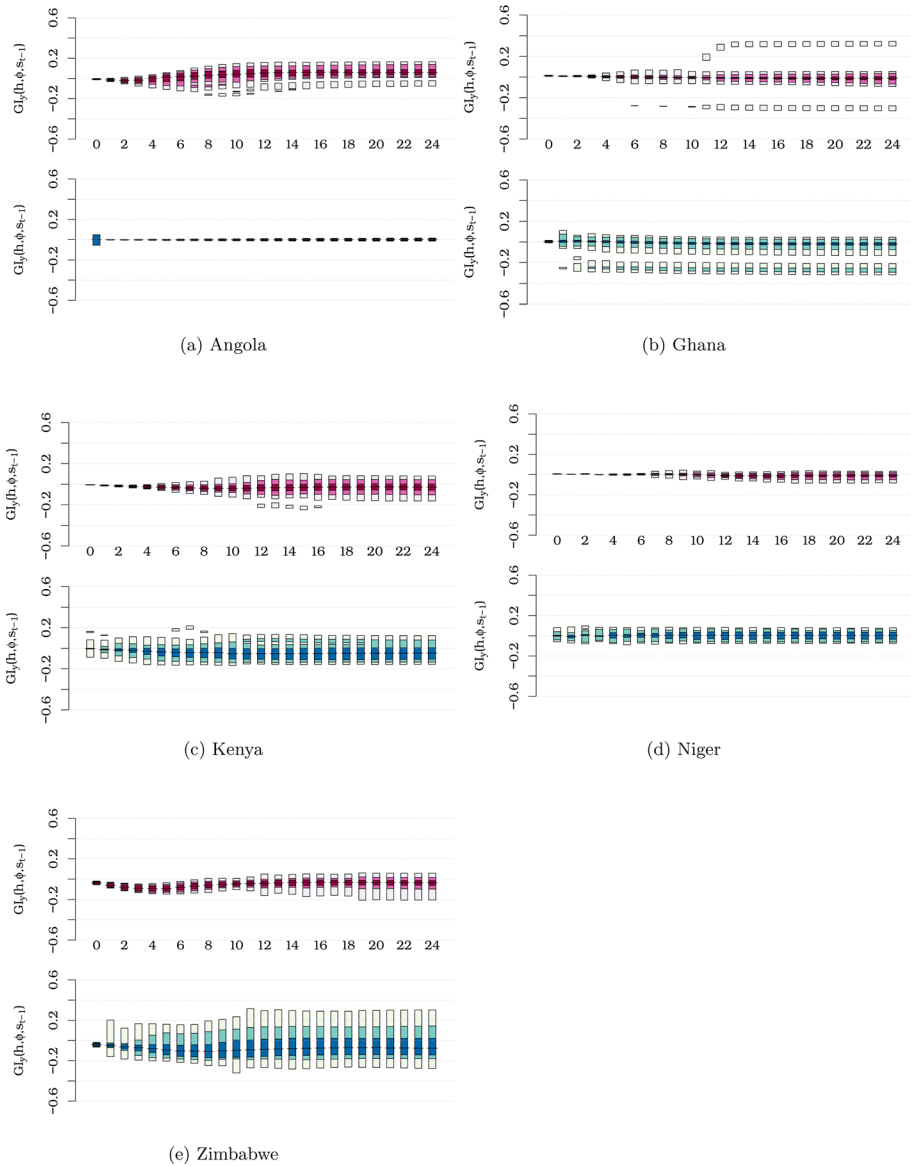
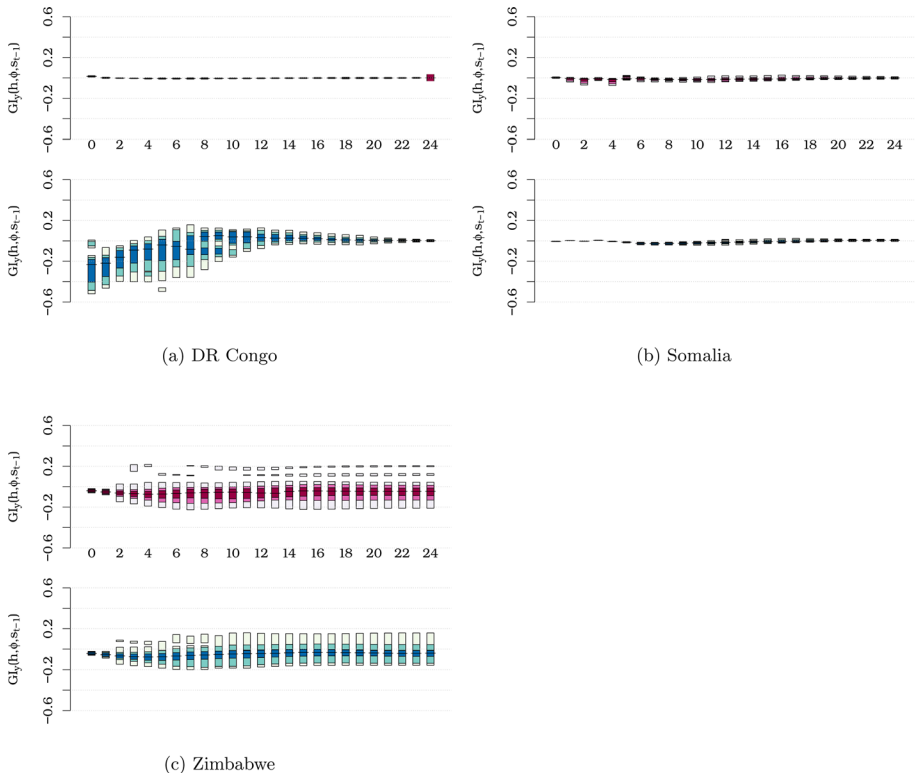**Fig. 7** Regime dependent asymmetry in maize prices. *Note*: The Figure features 50% (dark), 75% (fair) and 90% (light) highest density regions (HDRs) for generalized impulse response functions (GIRFs) in the non-linear two-regime STAR models. The GIRFs in each plot are associated with an average 1-standard deviation MEI shock during El Niño (upper panel) and La Niña (lower panel) regimes

to 8, are grouped into two classes. Figure 7 contains estimated GIRFs based on shocks emanating from *El Niño* and *La Niña* histories. On the other hand, Fig. 8 contains GIRFs estimated from histories before and after estimated structural shocks. It is essential to state that all the GIRFs are based on an average 1-standard deviation MEI shock.

(a) DR Congo

(b) Somalia

(c) Zimbabwe

Fig. 8 GIRFs of time-varying models of maize prices. *Note:* The Figure features 50% (dark), 75% (fair) and 90% (light) highest density regions (HDRs) for generalized impulse response functions (GIRFs) in the nonlinear two-regime STAR models. The GIRFs in each plot are associated with an average 1-standard deviation MEI shock before (upper panel) and after (lower panel) the respective estimated structural change

4.3.1 ENSO Regimes GIRFs

Figure 7 presents the price effects of MEI across ENSO regimes in countries where maize prices follow LSTARDL or LTV-LSTARDL processes - Angola, Ghana, Kenya, Niger, and Zimbabwe. Some general observations can be noted from the GIRFs. First, for most nonlinear series, the shocks have an amplified effect over time that appears to be more pronounced during *El Niño* seasons than in its counterpart season. However, these asymmetric effects appear to be reversed in Zimbabwe, a relatively cooler country. While the impact of a *La Niña* is negligible in Angola, the effect of an *El Niño* is weak in Niger. In Ghana, ENSO shock exerts an equally pronounced effect in both regimes. Generally, it is observed that the impact of an *El Niño* is subdued in West African countries than in other subregions, where the teleconnection effects are stronger.

Further, the impact of the shock is felt immediately in Zimbabwe, but after the fourth month in other countries. Specifically, introducing a one-standard-deviation positive MEI shock amplifies prices within the range of 2% to 20%. This impact is stronger for maize prices in Zimbabwe than other sampled countries. Another significant trend from the GIRFs is that the shock-induced effects do not seem to die out at the end of the period, thus showing persistence of these series. Finally, the uneven shapes of the HDRs in both

the upper and lower panels of the series suggest the existence of asymmetry between the two regimes - *El Niño* and *La Niña*. I also show a similar result based on season-specific *El Niño* and *La Niña* histories in Section C of the Appendix.

4.3.2 Time-Varying GIRFs

The last set of GIRFs considered is for those countries where maize prices are characterised by time-varying parameters: DR Congo, Somalia, and Zimbabwe.[34] Before considering the dynamic properties of these models, it is important to state that the countries where food prices are characterised by structural instability have a rich history of conflict, political instability, or local inequality (see, for instance, McGuirk and Burke 2020; Bellemare 2015). Moreover, most structural changes in food prices are induced by major ENSO phenomena. For example, the structural change in Somalia occurred around September 1998, coinciding with a major food crisis in the country due to extreme floods associated with ENSO activities (FAO 1998).

I now consider how the dynamic properties of these models change over time by computing their generalized impulses (GIs) before and after the estimated structural change. However, I will only compute ("unconditional") GI based on all histories before/after the structural change (see, section B of the Appendix for a detailed description of the GIRF calculation). Comparing the lower (pre-structural change) and upper (post-structural change) panels in Fig. 8, different traits are observed. For example, the effect of the shocks after the structural change is stronger than before the change for DR Congo, implying that food prices are more sensitive in the post-structural change era. Also, the impact after the structural change appears to die out from the 10th month. On the other hand, the shock effects appear to be equally spread out before and after the structural change for Zimbabwe while they are subdued in Somalia series.

4.4 Other Food Prices

In what follows, I consider other food prices with informative (non)linear ARDL model for SSA countries. The main results, together with the designated number of lags, the delay parameter and the selected model for each series, are summarised in Table A4 in the Appendix. Linearity is rejected against the STARDL model for most food prices in Angola, Burundi, Malawi, and Niger. In contrast, parameter stability is rejected against the TVARDL model for most food prices in Cameroon, DR Congo, and Eswatini. Moreover, the TV-STARDL is the preferred specification for few prices in Somalia and Zimbabwe, signifying a rejection of both linearity and parameter stability against Eq. (7).

Additionally, for all nonlinear models, the logistic function is preferred to the exponential function, with the exception of Eswatini (Bread) and Senegal (sorghum), where the ETVARDL model is preferred, and Malawi (imported rice), where ESTARDL is selected. Generally, most food prices in Eastern, Central and Southern Africa are influenced (either linearly or nonlinearly) by ENSO shocks (see Table A6 in the Appendix for a summary of model selection of each food price in SSA countries). These effects are, however, weak for most food prices in Western Africa, except for a few countries like Ghana and Niger. As a robustness check, I used SST and SOI instead of MEI as the transition variable and re-estimated the models. The results, which can be seen in Table A5 in the Appendix, portray

---

[34] Maize prices in Zimbabwe follow LTV-LSTARDL behaviour, as seen in Table 3.

much similarity to what is obtainable under the baseline specification: however, the choice of models is sensitive to the choice of transition variable for some food price series. I shall now analyse the rest of the price series by food classes. I avoid being detailed on the estimation and evaluation of these models, as the procedures have already been considered under the maize price series; hence this study will only apply itself to the choice of models.

4.4.1 Local and Imported Rice Prices

These two are paired together and separately from other grains to contrast their price behaviour. The map in Fig. 9 shows that most local rice prices follow an AR process (except Mali and Mozambique), whereas most imported rice series are shown to be affected by ENSO either linearly or nonlinearly. Two reasons can be put forward as to why ENSO shocks do not significantly affect local rice prices. First, much as rice is an important cereal crop in the region, it is a highly irrigated crop in SSA, unlike other rain-fed cereal crops. Thus, it is not vulnerable to local weather fluctuations (Schlenker and Lobell 2010). Second, most SSA economies (even in Western Africa, where large-scale production occurs) have yet to attain self-sufficiency in rice production. Therefore, to augment domestic needs, many rice-producing SSA countries import between 50% to 99% of their rice demand (FAO 2018). Consequently, the impact of ENSO on the prices of imported rice in SSA is rather indirect, passing through variation in production levels in exporting nations and then through international price volatility. For example, ENSO has been shown to have a profound impact on monsoonal rainfall across India and Thailand, the two biggest rice exporters (>50%), which in turn affect rice production in these economies (see, Wassmann et al. 2009; Singhrattna et al. 2005).

The character of the estimated models can be found in Table A4 and Figure A6 in the Appendix. No country's local rice price in my sample follows a nonlinear model. On the other hand, most of the nonlinear models of imported rice are STAR(DL) processes, while the rest allow for only structural changes.

4.4.2 Grain Prices

This subsection considers the general results from other food grain prices—millet, sorghum, and wheat. Majority of millet prices prefer an AR process (except in Niger and Ghana), as seen in Table A7 in the Appendix. This selection implies that millet prices in most SSA countries do not respond to ENSO occurrence as other cereal grain does, making it one of the most stable food prices in the region. Emediegwu et al. (2022); Wang et al. (2018) attribute this resistance characteristic to the physiological make-up of millet. For sorghum and wheat prices, the distribution of ENSO effects amongst countries is similar to maize prices, although Table A7 in the Appendix shows that the effect is more pronounced for sorghum prices than wheat prices. Unlike the result of the maize price series, the findings here suggest the effect of ENSO on sorghum is more felt in Western Africa than in other parts of Africa. The nature of the estimated models is displayed in Figure A7 in the Appendix.
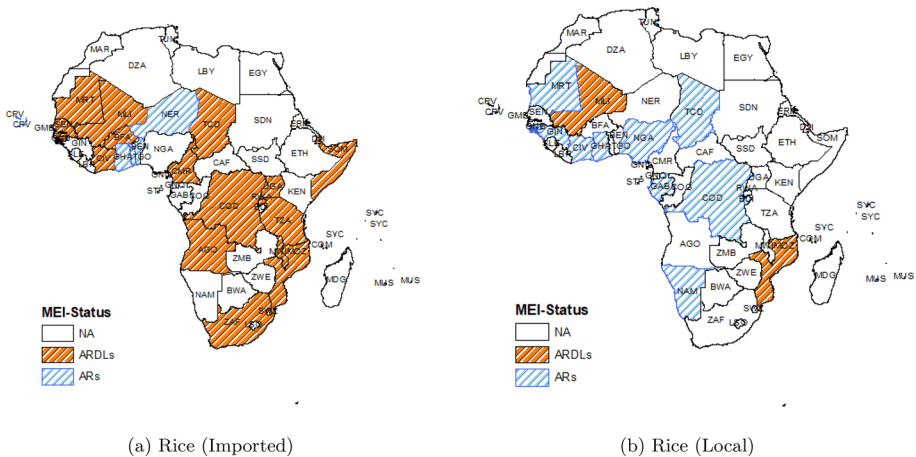
(a) Rice (Imported) (b) Rice (Local)

Fig. 9 Map of countries (un)affected by ENSO. *Note*: Yellow (blue) stripes are countries whose prices are (not) affected by ENSO shocks

4.4.3 Processed Food Prices

The price behaviour of processed food described in Table A7 in the Appendix is not very much different from those of staple foods like maize and sorghum. The selected models are equally distributed between AR and ARDL processes for all processed food in my sample, except for bread prices, where most of the models are ENSO dependent. There is a clear divide between smooth transition and time-varying model selection. For example, bread in Lesotho follows time-varying dynamics, while vegetable oil in the same country follows a smooth transition process between ENSO regimes, as shown in Figure A8 in the Appendix.

4.4.4 Animal Product Prices

Table A7 in the Appendix shows that food prices of animal origin are weakly affected by ENSO, excluding meat and milk prices in Kenya and Angola, respectively, which follow a smooth transition model, as displayed in Figure A9 in the Appendix. Climate change has been known to affect animal health. For instance, Walthall et al. (2012) show that a deviation of body temperature beyond 3°C could alter livestock's physiological behaviour, thereby affecting their performance and productivity. However, the extent to which this affects their prices has been debated. For example, prices of animal products are less volatile due to animals' abilities to adapt to marginal conditions and withstand shocks, making them good alternatives in the face of a changing climate (Gerber et al. 2013). Moreover, the stability of meat and milk prices in the face of ENSO shocks may be conditional on the stability of grain prices in some SSA countries.

4.4.5 The Rest

The last three food items - beans, cassava, and potato - can be classed as vegetables and roots. There is some degree of heterogeneity in the effect of ENSO on these price series. Table A7 and Figure A10 in the Appendix show that while crops such as cassava are ENSO tolerant, beans and potatoes appear to be ENSO sensitive. The resistance of cassava prices

to ENSO shocks can be attributed to the crops' physiological constituents, which fortify them against adverse meteorological events. For example, its deep root system allows it to withstand drought and can be grown in poor soils with low fertility, even after long periods of neglect (More et al. 2023). The paper's findings, therefore, agree with the notion that cassava, a climate-proof crop (see, FAO (2013)), can be used for adaptation purposes.

5 Summary and Policy Suggestions

This paper considers the regime-switching and structural instability of selected food prices in sub-Saharan Africa (SSA) using a time-varying smooth transition autoregressive (TV-STAR) model, as well as the extent to which ENSO (an exogenous climatic factor) influences food prices in the region. This study confirms a geographical and commodity dimension to the nature of the impact of ENSO on food prices in SSA, which is similar to the findings in Gaupp et al. (2020) in that correlation structure between the breadbaskets and the spatial dependence between climatic extremes globally can mitigate or aggravate the risks for the simultaneous failure of the global breadbasket. I find the impact of ENSO on maize prices to be more efficacious in Southern, Eastern, and some parts of Central Africa, while the effect is subdued in the Western African subregion. This finding confirms earlier studies that report a significant teleconnection effect in the highly affected subregions. The policy implication of this dichotomy is that response to ENSO news should be subregion- rather than region-specific, depending on how the subregions absorb the shock. Consequently, each subregional (economic) bloc in SSA must work out the most effective way to collectively respond to these natural phenomena.

Inter-regional trade might also increase price stability in the event of an ENSO. Countries where the teleconnection effects are not as strong can support those countries with strong teleconnection by cutting down cross-border trade barriers to improve trade flow of food commodities from areas of price stability to those of high price volatility.[35] However, in the face of the possibility of co-occurrence of climate crisis and other global crises (e.g., COVID-19, Russo-Ukrainian conflict) that can affect trade (see e.g., Laber et al. 2023; Falkendal et al. 2021; d'Amour and Anderson 2020), there is need for food import-dependent countries to anticipatorily plan against food shortages that might arise due to trade restrictions or reduction. Countries should adopt proactive risk management strategies that integrate climate adaptation, diversify food production, and ensure robust health and emergency response mechanisms during global emergencies. Besides, African nations must work together to tackle cross-border challenges and promote long-term climate resilience.

In terms of food products, the results find the effect of ENSO to be non-homogeneous across food prices. For example, imported rice and processed foods such as bread appear to be the most affected, while local rice, cassava, millet, and animal products like meat and milk are least affected. These results are not unexpected, given the physiological constituents of crops like millet and cassava that fortify them against adverse meteorological events. Consequently, some countries in the region, like DR Congo, are turning to these climate-resistant food commodities as a means of adapting to climate change (UNDP Climate 2017). On the other hand, since most SSA countries are

---

[35] While it is admitted that cutting down cross-border trade barriers may not be as easy as argued here due to supply and demand controls, it is possible with inter-regional cooperation and diplomatic dialogue.

import-dependent for rice and wheat (for making bread), the impact of ENSO on these prices in SSA is indirect, passing through variation in supply level in exporting nations. The effect of ENSO on prices of other food products, such as maize, sorghum, *etc.*, are evenly distributed across countries in the region.

This study has produced a regional model of how various food prices respond to climate anomalies. Given the wide coverage of countries and commodity classes in this study, the findings in this research provide policymakers and governments at national, sub-regional and regional levels in SSA some empirical basis to work with when determining how global climatic changes affect food prices. The detailed and robust number of price series considered will offer a microscopic view of how respective food prices are affected in various SSA countries; hence, decision-making can be formulated to tailor the commodity and country under consideration. This approach implies that a one-jacket solution may not fit all in response to climate issues. A detailed work like this is necessary to help relevant stakeholders understand how individual commodity prices are affected in various countries. For example, while some trends are common, such as the effect on imported rice, cassava, *etc.,* there are dissimilarities amongst others, such as maize, beans, *etc.* Furthermore, an in-depth understanding of price behaviour, especially from a climate perspective, will offer an opportunity for policymakers to manage food (in)security and adapt to climate change impacts, especially for the vulnerable, by detecting early warning signs.

Fluctuations in food prices have varying effects on producers and consumers, resulting in market dynamics that create winners and losers (see, e.g., Ludolph and Šedová 2021; McGuirk and Burke 2020). When food prices increase, producers typically benefit from increased revenues for their agricultural products. This is particularly true for producers with inelastic supply curves, who can capitalise on the higher prices without significantly increasing their production costs. On the other hand, consumers often encounter challenges as higher food prices strain on household budgets, particularly for low-income households that allocate a larger proportion of their income toward food expenses. This redistribution of welfare from consumers to producers can exacerbate tensions and result in various forms of conflicts, including social unrest, protests, and even violent conflicts, as witnessed in countries such as Tunisia and Egypt during the Arab Spring uprisings (Emediegwu 2022; Bellemare 2015). Therefore, it is essential to take appropriate measures to safeguard vulnerable populations from the negative effects of food price changes and address any potential social and economic imbalances that may arise.

The results in this paper indicate that, in the absence of mitigation or adaptation, global climate anomalies (such as ENSO) can lead to the end of "cheap food" in some parts of Africa. Moreover, the results in this paper show that certain crops, like cassava, millet, are better suited to withstand climate shock. These climate-resistant crops can be the food for the next century in developing regions in the face of the increasing frequency and intensity of climate anomalies. In addition to the adaptation strategies already mentioned, developing regions need to increase funds for research and development into means of fortifying and increasing the climate-resilience of " endangered" staple crops, which had hitherto suffered.

A caveat I must state is that food classes unaffected by global climate anomalies do not necessarily mean they have stable prices. It only means that climate does not affect them in any significant manner. For example, while this research shows that ENSO does not impact animal product prices, Von Braun et al. (2008) find that an increase in the purchasing power of middle-class consumers following rapid economic growth in certain developing countries results in a rise in prices of livestock products such as meat and milk. The

above scenario is one way of saying "no one jacket fits it all" as no single cause can fully explain all the dramatic changes in local (and global) food prices behaviour. The trends and activities seen are caused by interaction and interruption of several factors. While disentangling the individual effects of each channel is problematic, it will be a profitable venture to investigate which drivers are more active per region/country/food. For example, the principal drivers influencing food prices in Somalia might differ from those of Nigeria. And even within a country, the main drivers affecting maize prices might be different for those impacting milk prices. These disparities in driving forces could be an interesting area for further research.

References

Acemoglu D, Johnson S, Robinson JA (2001) The colonial origins of comparative development: an empirical investigation. Am Econ Rev 91(5):1369–1401

Agyei SK, Isshaq Z, Frimpong S, Adam AM, Bossman A, Asiamah O (2021) COVID-19 and food prices in sub-Saharan Africa. Afr Dev Rev 33:S102–S113

Ajanovic A (2011) Biofuels versus food production: Does biofuels production increase food prices? Energy 36(4):2070–2076

Balagtas JV, Holt MT (2009) The commodity terms of trade, unit roots, and nonlinear alternatives: a smooth transition approach. Am J Agr Econ 91(1):87–105

Bastianin A, Lanza A, Manera M (2016) 'Economic impacts of El Niño Southern Oscillation: evidence from the Colombian coffee market', *Centro Euro-Mediterraneo per i Cambiamenti Climatici (CMCC)*

Bazzi S, Blattman C (2014) Economic shocks and conflict: evidence from commodity prices. Am Econ J Macroecon 6(4):1–38

Bellemare MF (2015) Rising food prices, food price volatility, and social unrest. Am J Agr Econ 97(1):1–21

Blanc E, Reilly J (2017) Approaches to assessing climate change impacts on agriculture: an overview of the debate. Rev Environ Econ Policy 11(2):247–257

Brunner AD (2002) El Nino and world primary commodity prices: Warm water or hot air? Rev Econ Stat 84(1):176–183

Callahan CW, Mankin JS (2023) Persistent effect of El Niño on global economic growth. Science 380(6649):1064–1069

Cashin P, Mohaddes K, Raissi M (2017) Fair weather or foul? The Macroeconomic effects of El Niño. J Int Econ 106:37–54

CIESIN (2018), *Gridded Population of the World, Version 4 (GPWv4): Population Count, Revision 11*, Palisades, NY: NASA Socioeconomic Data and Applications Center (SEDAC)

Cottrell RS, Nash KL, Halpern BS, Remenyi TA, Corney SP, Fleming A, Fulton EA, Hornborg S, Johne A, Watson RA et al (2019) Food production shocks across land and sea. Nat Sustain 2(2):130–137

d'Amour CB, Anderson W (2020) International trade and the stability of food supplies in the Global South. Environ Res Lett 15(7):074005

d'Amour CB, Wenz L, Kalkuhl M, Steckel JC, Creutzig F (2016) Teleconnected food supply shocks. Environ Res Lett 11(3):035007

Deaton A (1999) Commodity prices and growth in Africa. J Econ Perspect 13(3):23–40

Deaton A, Laroque G (1992) On the behaviour of commodity prices. Rev Econ Stud 59(1):1–23

Deaton A, Laroque G (1996) Competitive storage and commodity price dynamics. J Polit Econ 104(5):896–923

Dell M, Jones BF, Olken BA (2012) Temperature shocks and economic growth: evidence from the last half century. Am Econ J Macroecon 4(3):66–95

Dillon BM, Barrett CB (2015) Global oil prices and local food prices: evidence from East Africa. Am J Agr Econ 98(1):154–171

Emediegwu LE (2022) 'How is the war in Ukraine affecting global food prices?'. https://www.economicso bservatory.com/how-is-the-war-in-ukraine-affecting-global-food-prices/ (accessed June 14, 2022)

Emediegwu LE, Nnadozie OO (2022) On the effects of COVID-19 on food prices in India: a time-varying approach. Eur Rev Agric Econ 50(2):232–249

Emediegwu LE, Rogna M (2024) Agricultural commodities' price transmission from international to local markets in developing countries. Food Policy 126:102652

Emediegwu LE, Ubabukoh CL (2023) Re-examining the impact of annual weather fluctuations on global livestock production. Ecol Econ 204:107662

Emediegwu LE, Wossink A, Hall A (2022) The impacts of climate change on agriculture in sub-Saharan Africa: a spatial panel data approach. World Dev 158:105967

Falkendal T, Otto C, Schewe J, Jägermeyr J, Konar M, Kummu M, Watkins B, Puma MJ (2021) Grain export restrictions during covid-19 risk food insecurity in many low-and middle-income countries. Nat Food 2(1):11–14

FAO (1998) FAO'S special report on sub-Saharan Africa: improved outlook forecast for much of sub-region; but Somalia faces severe food shortages and civil strife threatens food supplies in Democratic Republic Of Congo, FAO, Rome

FAO (2013) Save and Grow: Cassava—a guide to sustainable production intensification. FAO, Rome

FAO (2017) Global report on food crisis 2017. FAO, Rome

FAO, IFAD, UNICEF, WFP & WHO (2018), The State of Food Security and Nutrition in the World 2018: building climate resilience for food security and nutrition, FAO Rome

Fowowe B (2016) Do oil prices drive agricultural commodity prices? Evidence from South Africa. Energy 104:149–157

Gaupp F, Hall J, Hochrainer-Stigler S, Dadson S (2020) Changing risks of simultaneous global breadbasket failure. Nat Clim Chang 10(1):54–57

Gerber PJ, Steinfeld H, Henderson B, Mottet A, Opio C, Dijkman J, Falcucci A, Tempio G. et al. (2013) Tackling climate change through livestock: a global assessment of emissions and mitigation opportunities., Food and Agriculture Organization of the United Nations (FAO), Rome

Gilbert CL, Morgan CW (2010) Food price volatility. Philos Trans R Soc B Biol Sci 365(1554):3023–3034

Granger CW (1993) Strategies for modelling nonlinear time-series relationships. Econ Rec 69(3):233–238

Granger CW, Terasvirta T et al (1993) Modelling non-linear economic relationships. OUP Catalogue. Oxford University Press, Oxofrd

Harari M, Ferrara EL (2018) Conflict, climate, and cells: a disaggregated analysis. Rev Econ Stat 100(4):594–608

Headey D, Fan S (2008) Anatomy of a crisis: the causes and consequences of surging food prices. Agric Econ 39:375–391

Hsiang S (2016) Climate econometrics. Annu Rev Res Econ 8:43–75

Hsiang SM, Meng KC (2015) Tropical Economics. Am Econ Rev 105(5):257–61

Hsiang SM, Meng KC, Cane MA (2011) Civil conflicts are associated with the global climate. Nature 476(7361):438

Hyndman RJ (1995) Highest-density forecast regions for nonlinear and non-normal time series models. J Forecast 14(5):431–441

Hyndman RJ (1996) Computing and graphing highest density regions. Am Stat 50(2):120–126

Iizumi T, Ramankutty N (2015) How do weather and climate influence cropping area and intensity? Glob Food Sec 4:46–50

Tabe-Ojong JR, Paul M, Nshakira-Rukundo E, Haile Gebrekidan B (2023) COVID-19 and food insecurity in Africa: a review of the emerging empirical evidence. Eur Rev Agric Econ 50(3):853–878

Kargbo JM (2000) Impacts of monetary and macroeconomic factors on food prices in Eastern and Southern Africa. Appl Econ 32(11):1373–1389

Keppenne CL (1995) An ENSO signal in soybean futures prices. J Clim 8(6):1685–1689

Koop G, Pesaran MH, Potter SM (1996) Impulse response analysis in nonlinear multivariate models. J Econ 74(1):119–147

Laber M, Klimek P, Bruckner M, Yang L, Thurner S (2023) Shock propagation from the Russia-Ukraine conflict on international multilayer food production network determines global food availability. Nat Food 4(6):508–517

Letson D, McCullough B et al (2001) ENSO and soybean prices: correlation without causality. J Agric Appl Econ 33(3):513–522

Ludolph L, Šedová B (2021) Global food prices, local weather and migration in Sub-Saharan Africa. Technical report, Center for Economic Policy Analysis

Lundbergh S, Teräsvirta T, Van Dijk D (2003) Time-varying smooth transition autoregressive models. J Bus Econ Stat 21(1):104–121

McArthur J, Sachs JD (2001) 'Institutions and Geography: comment on Acemoglu, Johnson and Robinson (2000)', *NBER Working Paper* (w8114)

McGuirk E, Burke M (2020) The economic origins of conflict in Africa. J Polit Econ 128(10):3940–3997

Minot N (2014) Food price volatility in Sub-Saharan Africa: Has it really increased? Food Policy 45:45–56

More SJ, Bardhan K, Ravi V, Pasala R, Chaturvedi AK, Lal MK, Siddique KH (2023) Morphophysiological responses and tolerance mechanisms in cassava (Manihot esculenta Crantz) under drought stress. J Soil Sci Plant Nutr 23(1):71–91

Narciso G (2020) Reprint of: crop prices and the individual decision to migrate. Food Policy 94:101884

Raleigh C, Choi HJ, Kniveton D (2015) The devil is in the details: an investigation of the relationships between conflict, food price and climate across Africa. Glob Environ Chang 32:187–199

Schlenker W, Lobell DB (2010) Robust negative impacts of climate change on African agriculture. Environ Res Lett 5(1):1–8

Singhrattna N, Rajagopalan B, Clark M, Krishna Kumar K (2005) Seasonal forecasting of Thailand summer monsoon rainfall. Int J Climatol J R Meteorol Soc 25(5):649–664

Smith SC, Ubilava D (2017) The El Niño Southern Oscillation and economic growth in the developing world. Glob Environ Chang 45:151–164

Teräsvirta T (1994) Specification, estimation, and evaluation of smooth transition autoregressive models. J Am Stat Assoc 89(425):208–218

Tong H (1990) Non-linear Time Series: a Dynamical System Approach. Oxford University Press, Oxford

Tsay RS (1989) Testing and modeling threshold autoregressive processes. J Am Stat Assoc 84(405):231–240

Ubilava D (2017) The role of El Nino Southern Oscillation in commodity price movement and predictability. Am J Agr Econ 100(1):239–263

Ubilava D, Abdolrahimi M (2019) The El Niño impact on maize yields is amplified in lower income teleconnected countries. Environ Res Lett 14(5):054008

UN (2017a), 'Report of the Secretary-General, "Progress towards the Sustainable Development Goals", E/2017/66'

UN (2017b), 'The Sustainable Development Goals Report 2017'. https://unstats.un.org/sdgs/files/report/2017/TheSustainableDevelopment-GoalsReport2017.pdf/ (accessed May 7, 2018)

UNDP Climate (2017), 'THE MAGIC OF CASSAVA: Adapting to climate change in the Democratic Republic of the Congo'. https://undp-climate.exposure.co/the-magic-of-cassava/ (accessed May 7, 2018)

Van Dijk D, Teräsvirta T, Franses PH (2002) Smooth transition autoregressive models: a survey of recent developments. Economet Rev 21(1):1–47

Von Braun J, Ahmed A, Asenso-Okyere K, Fan S, Gulati A, Hoddinott J, Pandya-Lorch R, Rosegrant M, Ruel M, Torero M, Van Rheenen T, Von Grebmer K (2008) Rising Food Prices: What Should Be Done? International Food Policy Research Institute, Washington, D.C

Walthall C, Hatfield J, Backlund P, Lengnick L, Marshall E, Walsh M, Adkins S, Aillery M, Ainsworth E, Ammann C. et al. (2012) 'Climate change and agriculture in the United States: Effects and adaptation. USDA Technical Bulletin 1935. Washington, DC', *US Department of Agriculture*

Wang J, Vanga S, Saxena R, Orsat V, Raghavan V (2018) Effect of climate change on the yield of cereal crops: a review. Climate 6(2):41

Wassmann R, Jagadish S, Sumfleth K, Pathak H, Howell G, Ismail A, Serraj R, Redona E, Singh R, Heuer S (2009) Regional vulnerability of climate change impacts on Asian rice production and scope for adaptation. Adv Agron 102:91–133

Wheeler T, Von Braun J (2013) Climate change impacts on global food security. Science 341(6145):508–513

Wolter K (1993) Monitoring ENSO in COADS with a seasonally adjusted principal component index, In: *Proceedings of the 17th Climate Diagnostics Workshop*, 1993

Zhang Z, Lohr L, Escalante C, Wetzstein M (2010) Food versus fuel: What do prices tell us? Energy Policy 38(1):445–451